Numerical Methods in Civil Engineering

Force Reduction Factor R for Shear Dominated Low-Rise Brick Masonry Structures

Naveed Ahmad[*], Qaisar Ali[**], and Muhammad Javed[***]

ARTICLE INFO

Article history:
Received:
October 2017.
Revised:
December 2017.
Accepted:
March 2018.

Keywords:
Brick masonry; Behavior Factor; Seismic Response Modification Factor; Masonry Shear Walls

Abstract:

This paper presents investigation carried out, including experimental and numerical studies, on low-rise shear-dominated brick masonry structures for the calculation of force reduction factor R. Basic experimental tests were conducted on masonry constituent materials for mechancial characterization. In-plane quasi-static cyclic tests were conducted on twelve full scale brick masonry walls, to understand behavior of shear-dominated walls under in-plane lateral loads. The tests' data were analyzed to obtain the lateral shear strength, elastic and inelastic displacement capacities and hysteretic response of walls to facilitate numerical modelling of masonry structures. The numerical study included incremental dynamic analyses of shear-dominated brick masonry structures for the derivation of structures' response curves, correlating the ground motion severity with the inelastic displacement demand on structure. The ductility dependent R factor is computed by identifying the ground motion intensities: capable to initiate global yielding in the structure (PGAy) and that exceeding the limit state displacement capacity of structure (PGAu), respectively. The ratio of the two PGAu/PGAy provides estimate of structures' R factor. The calculated R factor varies in the range of 1.20 to 2.74, with a mean of 1.64; 1.5 may be conservatively used in the design and assessment of considered structures.

1. Introduction

Earthquake observations have revealed that masonry structures meeting the minimum requirements to ensure in-plane wall resistance for earthquake induced lateral load, and those designed with modest efforts have performed significantly well; ensuring the safety of occupants during damaging earthquakes (Ahmad, 2015; Ali, 2007; Jackson, 1960; Jain and Nigan, 2000; Kumar, 1933; Dizhur et al., 2010 & 2011; Senaldi et al., 2014). Recent experiences have shown that ordinary masonry structures designed to meet the minimum requirements of earthquake resistant structures can avoid total structural collapse and consequently fulfill the objective of collapse prevention during very large rare earthquakes (Magenes, 2006; Tomazevic, 1999). Also, affordable strengthening techniques like floor stiffening to avoid out-of-plane walls deflection (Klinger, 2004) can enable masonry structure resist ground motions even up to peak ground acceleration of 0.70g (Magenes et al., 2013, Penna et al., 2015; Senaldi et al., 2014). Shear-dominated unreinforced masonry structures employing good quality materials i.e. high strength unit and mortar, and constructed using basic engineering principles; load bearing walls constructed in proper bond achieving good wall-to-wall connection through practicing toothed joints and the building is provided with rigidly connected floor (Murthy, 2005), can withstand ground shaking intensity up to 0.70g (Ali and Naeem, 2007; Ali et al., 2012a).

All the above confirm that there exist significant deformability and energy dissipation in masonry structures beyond the initial cracking that is playing rule to resist moderate earthquake event, and even possibly larger earthquake events. This points to the need for investigation of masonry structures, particularly those confirming to the minimum requirements to offer lateral resistance through global in-plane response and avoid the local out-of-plane failure of walls. It is worth to facilitate simplified elastic procedures for the design and assessment of such structures, especially in moderate to high seismicity

**Corresponding Author: Postgraduate Advisor of Earthquake Engineering, Department of Civil Engineering, UET Peshawar. naveed.ahmad@uetpeshawar.edu.pk*

regions. For regions with very high seismicity, additional provisions will be required to withstand severe ground motions e.g. providing lightly reinforced horizontal bands and confining columns in load bearing walls (Shahzada et al., 2011). These additional provisions when practiced even in low-strength structure (like rubble masonry) can significantly enhance its seismic resistance to withstand against simulated earthquake motions of moderate to high seismicity regions (Ali et al., 2013).

This research presents investigation carried out on the seismic performance assessment of low-rise shear-dominated brick masonry structures in the northern regions of Pakistan. The considered structures composed of loadbearing walls built in solid clay units and cement-sand-khaka mortar for construction, practiced with deep spandrels, which are provided with rigid reinforced concrete floor as common in the urban exposures of Pakistan (see Figure 1). Khaka is obtained as a byproduct of stone crushing process, when employed in mortar preparation produces relatively workable, economical and high strength mortar (Naeem et al., 1996; Ali et al., 2012b; Alsuwwi et al., 2015).

Three Storey Unreifnroced Brick Masonry Building

Damages in Brick Masonry Buildings in 2005 Kashmir Earthquake

Fig. 1: Typical brick masonry constructions in Pakistan and observed behavior during damaging earthquakes.

Experimental investigations were carried out for masonry materials characterization (Ali et al., 2012b, Alsuwwi et al., 2015), to understand the basic mechanical properties of masonry material, and in-plane shear strength evaluation of full-scale shear-dominated masonry walls (Javed et al., 2015) to help in the development and calibration of numerical modeling of similar like structures. Forty-nine (49) case study numerical models were considered which were analyzed;

(a) First, using nonlinear static pushover analysis to obtain the lateral force-deformation capacity curve of structures (to identify the structure deformation capacity at the yielding and ultimate limit state) and

(b) Second, employing nonlinear dynamic time history analysis for the derivation of structure response curves (correlating the intensity level with the deformation demand on the structure) for the estimation of response modification factor R of shear-dominated masonry structures.

The experimental data retrieved from the cyclic response of in-plane full scale shear walls were considered to calibrate the hysteretic constitutive law of masonry wall, which was tested and validated to simulate reasonably the lateral load-displacement response of tested masonry walls. The data was also analyzed to generalize the wall constitutive law for possible extension to shear-dominated brick masonry walls of varying geometry and pre-compression level. The R factor is calculated through nonlinear dynamic time history analysis (NLTHA) in order to truly capture the hysteretic energy dissipation capacity of the structure (as recommended elsewhere e.g. Kappos, 1999; Porto et al., 2009; FEMA P-695, 2009) besides taking into account the record-to-record variability of ground motions in structures' seismic performance evaluation.

2. Response Modification Factor R

The response modification factor R in the current building code of Pakistan has been adopted from the UBC-97, that takes into account the inherent over strength in the structure (lateral shear strength of structure in excess to the design shear force demand) and global ductility capacity of lateral force-resisting systems. A force reduction factor of 4.5 is recommended for shear wall masonry buildings. This included overstrength of 2.80 and a ductility factor of 1.60.

It is worth to mention that the importance of energy dissipation capacity due to nonlinear behavior of structure is not considered by the code but rather it is referred to the ductility factor computed using the energy balance rule multiplied by the structural over strength. It has been demonstrated that structural systems with similar stiffness and strength can result in different inelastic deformation demand, and hence different performance state, considering different nonlinear hysteretic behavior (Priestley et al., 2007; FEMA P-695, 2009). It is due to the fact that different level of energy dissipation capacity is assigned to

the system, which is not explicitly addressed. This fact makes essential to estimate construction specific R factor for various load resisting systems e.g. buildings employing different masonry materials and construction practices that can affect the energy dissipation capacity of the system besides may also affect stiffness, strength and ductility of the structure. A number of studies conducted on various structural systems have highlighted the importance of structures' specific R factor (Mahmoudi and Zaree, 2013; Masoudi et al., 2012). The present research is thus essential to calculate R factor for shear-dominated masonry structures and propose R factor for simplified design and assessment procedures.

The R factor is the ratio of the seismic force the structure would experience if its response was completely elastic in the design level earthquake to the minimum seismic force that may be used in the design still ensuring a satisfactory response of the structure. The structure if designed to this minimum seismic force, the target deformation capacity of the structure will not be exceeded during ground motions of the design level earthquake (Miranda, 1997; Kappos, 1999). It is formulated as follows :

$$R = \frac{F_e}{F_d} \tag{1}$$

where F_e represents the elastic force demand for the structure deemed to respond elastically to the earthquake. Using the code-specified acceleration spectrum, it can be calculated by obtaining the spectral acceleration at the fundamental vibration period of the structure, which is multiplied by the seismic mass of the structure. F_d represents the minimum strength that may be employed in the design of structure such that the structure does not exceed the specified deformation capacity in the design level earthquake.

Generally, R factor mainly depend on the ductility and energy dissipation capacity of structure, on the strength reserves that depends on the structure redundancy and on the over strength of individual members, and on the effective damping of the structure. All these factors directly affect the energy dissipation capacity of a structure (Kappos, 1999), whereby R factor can be formulated as given below :

$$R = R_\mu R_s R_\xi \tag{2}$$

where R_μ represents the ductility dependent component; R_s represents the over strength dependent component. It is the ratio of the maximum strength of the system to the minimum design force, also called as the over strength ratio OSR (Magenes, 2004). $R\xi$ represents the damping dependent component in case of structure with supplemental damping devices.

The ductility dependent component may be obtained best through techniques capable of truly capturing the energy dissipation capacity of the structure e.g. NLTHA. In this regard, a true nonlinear hysteretic behavior of structural elements is crucial (Kappos, 1999; Porto et al., 2009; FEMA P-695, 2009). NLTHA also have the advantage to capture the record-to-record variability impact on the structure response. More generally, the energy balance criterion and the classical analytical model, is used to compute Rμ for masonry structures, however, this approach does not differentiate in the reduction factor for systems having similar stiffness, strength and ductility but distinct hysteretic behavior. Because, the hysteretic response can significantly affect the seismic demand and the expected performance of structures during earthquakes (Priestley et al., 2007; FEMA P-695, 2009).

The system over strength dependent Rs factor can be best obtained carrying out nonlinear static pushover analysis of the structure in order to estimate the maximum lateral strength of the system and the force corresponding to the minimum design level force (Magenes and Morandi, 2008, Morandi and Magenes, 2008). However the estimation of Rs is not very straight forward and is highly influenced by the actual structural configuration, distribution of seismic forces in the plan of structures i.e. to individual walls, in-plane rigidity/flexibility of structure floors and the means of wall coupling (e.g. weak/strong spandrels, ring beams, tie rods, etc.). The above facts clearly indicate that experimental investigation alone cannot give a realistic estimate of R factor in general and the use of numerical techniques along with the experimental findings may be best used, thereof.

3. Experimental Program

Almost all masonry typologies found in Pakistan have been subjected to high-to-strong ground motions during earthquake events in the near past (Ahmad, 2015; Javed et al., 2008; Rossetto and Peiris, 2009). However, such earthquake observations are not sufficient for understanding the design parameters (i.e. response modification factor) of the damaged structures to facilitate design and assessment of new constructions. Numerous experimental investigations have been carried out on masonry materials (Ali and Naeem, 2007; Ali et al., 2012a, 2012b; Alsuwwi et al., 2015; Shahzada et al., 2012), however, these studies primarily focused on characterization of mechanical properties of masonry material at the micro levels (i.e. units, bonding materials, masonry assemblages, etc.) or a global performance assessment of the whole structure, which do not provide complete information to help in numerical modelling of shear-dominated masonry structures for dynamic seismic analysis and computation of structure specific R factor. Thus, the experimental study in this research included in-plane quasi-static cyclic tests on shear-dominated masonry walls to help understand their in-plane cyclic response, holistically. The aim of the quasi-static cyclic tests was to retrieve the lateral stiffness and strength, force-deformability and hysteretic behavior of walls, understand the damage mechanism of walls and deduce performance limits for deformation-based assessment of shear-dominated masonry wall structures. These properties provided help in numerical modelling and dynamic seismic analysis of masonry structures, for the estimation of R factor of considered structures.

The experimental program also included tests on constituent materials and masonry assemblages to obtain the basic properties of masonry materials. It was essential for two reasons: (a) First, to obtain the desired masonry materials as practiced in the field (Ali and Naeem, 2007) and (b) Second, to retrieve the basic mechanical properties to help in facilitating analytical models used for estimation of in-plane shear strength of masonry walls (Abrams, 2001; CEN, 1994; FEMA, 2000; Magenes and Calvi, 1997; Mann and Muller, 1982; Tomazevic, 1999; Turnsek and Sheppard, 1980).

Quasi-static in-plane cyclic tests were performed on twelve (12) full-scale load-bearing walls. The walls under consideration included brick masonry walls of aforementioned masonry and built in English bond type, representing the residential building construction practice in the northern urban areas of Pakistan (Ali and Naeem, 2007; Javed, 2008; Javed et al., 2015; Alsuwwi et al., 2015). The test specimens were consisted of four series of walls with varying geometric and loading conditions to help simulate the most likely cases of loadbearing walls in shear-dominated buildings (Table 1).

Table 1. Characteristics of wall specimens considered for in-plane quasi-static cyclic tests, after Javed et al. (2015)

S. No.	Walls	Aspect Ratio*	Pre-Compression*	Description
1	Three	0.66	0.138	**Wall-1:** It represents the effective dimensions (effective height and width) of masonry pier for room walls having opening for a door at one side. The pre-compression represents the gravity loading on walls in two-to-three storey buildings.
2	Three	0.93	0.138	**Wall-2:** It represents the effective dimensions (effective height and width) of masonry pier for room walls having opening for a door at one side. The pre-compression represents the gravity loading on walls in two-to-three storey buildings.
3	Three	0.93	0.091	**Wall-3:** It represents the effective dimensions (effective height and width) of masonry pier for room walls having opening for a door at one side. The pre-compression represents the gravity loading on walls in two-to-three storey buildings.
4	Three	1.22	0.153	**Wall-4:** It represents the effective dimensions (effective height and width) of masonry pier for room walls having opening at both sides. The pre-compression represents the gravity loading on walls in two-to-three storey buildings.

Aspect ratio (H/D) refers to the wall height-to-length ratio; H and D represent the height and length of wall respectively.
Pre-compression (σ/f_m) represents the intensity of axial stress (σ) on the wall due to gravity loading.

The in-plane walls were fixed both at the bottom and top ends and connected to a lateral loading rigid frame (Figure 2). The setup was provisioned with vertically applied two hydraulic jacks having steel rollers, to subject the specimen to a specified pre-compression yet allowing lateral movement of the test specimen. The test specimens were instrumented with displacement transducers (i.e. LVDTs connected to data acquisition system for recording), to measure lateral horizontal displacement, specimen rotation, and specimen diagonal deformation, to help obtain the relative in-plane horizontal deformation of the specimens.

The in-plane lateral loading protocol consisted of force-controlled and displacement-controlled cyclic time history, applied on specimen at the top by means of rigid frame (pushed back and forth by hydraulic actuator). The force-controlled regime included four target force levels (i.e. 1/4, 1/2, 3/4,1) of a specified lateral force that was 75% of the analytically estimated lateral force capacity of specimen using the available simplified shear strength models (Tomazevic, 1999), each applied in three cycles. In the displacement-controlled regime, the maximum lateral displacement observed in the force-controlled phase was considered as a reference, the lateral target displacement were increased gradually with an increment of 0.254 mm, which is applied in three cycles with 120 Hz frequency, till extensive damages were observed in the specimen or when the test specimen was found to be unstable, whereby the test was stopped.

In the first force-controlled phase of the test, inelasticity was developed in all the tested walls; primarily diagonal tension cracks were initiated at the end of this phase test. In the second displacement-controlled phase of the test, the already developed cracks were aggravated and additional crack lines were also initiated leading to severe damage in walls and local/global instability. All the tested walls primarily exhibited diagonal tension cracking through mortar head-/bed-joint (well distributed over the wall surface in case of relatively high pre-compression and localized in case of lower pre-compression), it is followed by masonry crushing at the compressed toe (in case of slender walls) or horizontal bed-joint sliding and masonry splitting, in case of squat walls, (Figure 3).

The force and deformation recorded during test were stored in the acquisition system and processed (after essential signal 0.10 Hz low pass filtering and smoothing through moving average filtering) to retrieve essential response parameters including the force-deformation hysteretic response; average lateral force-deformation curve; and hysteretic energy dissipation in walls at various performance levels, as per the available recommendations (Javed et al., 2015; Magenes and Calvi, 1997; Vasconcelos and Lourenco, 2009). From Figure 4, it can be observed in

all specimens that significant inelasticity develop in a wall soon after the appearance of first crack, which either occurred earlier than the first diagonal crack (in case of slender walls and walls with low pre-compression) or occurred simultaneously with diagonal cracking (in case of squat walls and walls with high pre-compression). The deformability capacity is relative more in case of slender walls but also in squat walls with high pre-compression when localized failure was avoided and sliding was ensured. The energy dissipation capacity is relative lower in case of slender walls, while significant in case of squat walls with low pre-compression and very larger in case of very squat walls with sliding phenomenon.

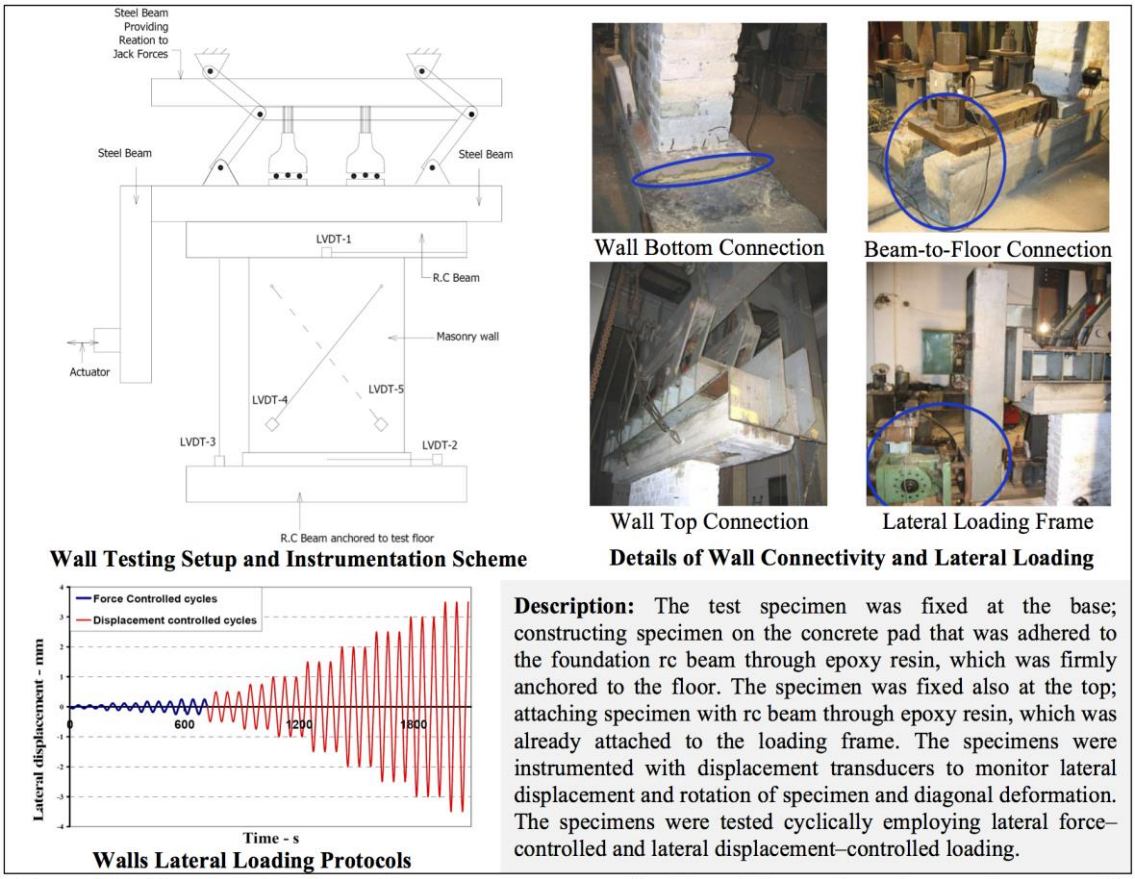

Fig. 2: In-Plane quasi-static cyclic test on masonry walls, after Javed et al. (2015)

4. Description of Brick Masonry Structures

The present study considered forty-nine (49) low-rise (two-storey) structures for the seismic performance assessment and computation of R factor. Figure 5 shows the geometry of the considered structures investigated in the present research study. These structures are designed to meet the geometric and material characteristics of urban brick masonry residential buildings in northern Pakistan, and to ensure shear damage mechanism.

These structures employ 230 mm thick load bearing walls constructed of solid clay units and cement-sand-khaka mortar in English bond type. These structures are provided with rigid reinforced concrete slab floors. An inter-storey height of 3.0m to 3.5m is considered for first storey and 2.50m to 3.0m is considered for second storey.

The load bearing walls are perforated by doors and windows of varying width and fixed height and considered with deep spandrels of 1.0m (in most common cases) to 1.50m (in few rare cases). The predominant seismic resistance mechanism for this configuration, as observed in the dynamic test (Ali and Naeem, 2007) and earthquake observation (Ahmad, 2015; Javed et al., 2015, Peiris et al., 2008; Naseer et al., 2010) is in-plane mechanism with shear damage of masonry walls. The current field practice is to employ also ring beam, lintel and plinth level bands, which will consequently reduce the wall slenderness. It will consequently ensure in-plane integrity of structures during earthquake excitations that mostly result into the shear mechanism of in-plane walls under lateral loads.

Wall Series	Observed Progressive Damage Mechanism *Slight to Moderate to Extensive Damage States*
Wall–1 (W1)	 **Description:** Test specimen of this type represented very squat walls found in residential buildings. The overall damage mechanism in these types of walls is found to be diagonal tension failure of masonry followed by bed-joint sliding. These type of walls when subjected to low pre-compression result in multiple diagonal cracks and vertical cracks passing through mortar head- and bed-joints that is followed by horizontal cracks along the bed-joint. These walls if stressed with high pre-compression level result in diagonal cracks passing mortar joints and brick units that is followed by horizontal bed-joint sliding and masonry splitting.
Wall–2 (W2)	 **Description:** Test specimen of this type also represented squat walls found in residential buildings wall having one or no opening. These walls showed diagonal tension failure of masonry in a more prominent fashion, well distributed over the whole surface of the wall, with diagonal cracks passing through mortar head- and bed-joints, unlike W1, the subsequent horizontal bed-joint sliding was not observed and the masonry splitting was rare and less severe.
Wall–3 (W3)	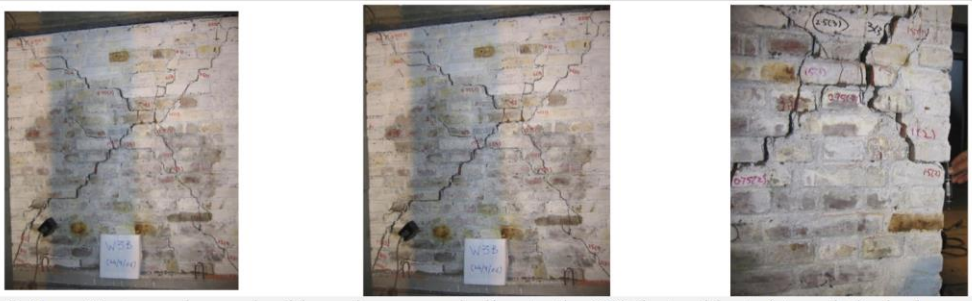 **Description:** Test specimens in this series were similar to the W2 but subjected to relatively lower pre-compression. These wall types showed diagonal tension failure of masonry with cracks passing mortar head- and bed-joints. However, unlike W2, the diagonal cracks were not well distributed over the wall surface but rather localized at one side of the wall that resulted in the detachment of wedge-like masonry. This damage localization is due to the relatively low level of pre-compression.
Wall–4 (W4)	 **Description:** Test specimen of this type represented slender walls found in residential buildings walls having opening on either side. The overall damage mechanism observed in these types of walls included diagonal tension failure of masonry, through the formation of few diagonal crack lines, followed by masonry crushing at compressed toe. The observed diagonal cracks passed through mortar head- and bed-joint.

Fig. 3: Observed behavior of shear-dominated masonry walls under in-plane lateral quasi-static cyclic tests

Walls	Hysteretic Response	Idealized Force-Deformation	Energy Dissipation	Description
W1	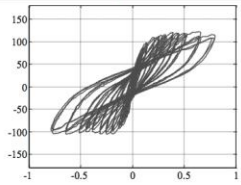	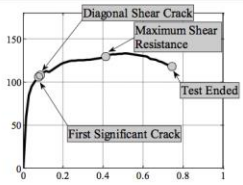	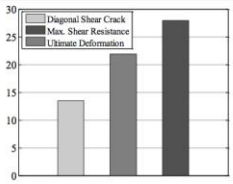	Specimen in this series showed high strength and very stable response, the lateral strength started dropping when sliding was following by localized masonry splitting. The specimens possessed very high energy dissipation capacity, due to sliding mechanism.
W2	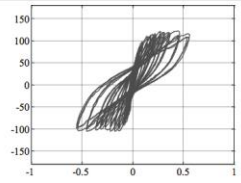	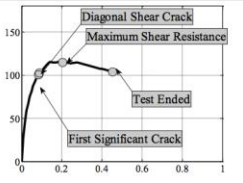	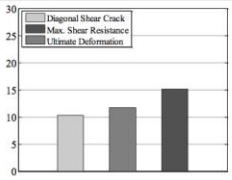	Specimen in this series also showed very stable response, the lateral strength started dropping due to localized masonry splitting. These specimens also possessed significant energy dissipation capacity, due to multiple diagonal cracks.
W3	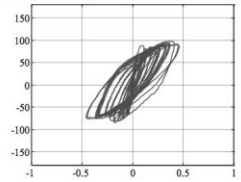	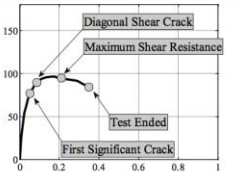	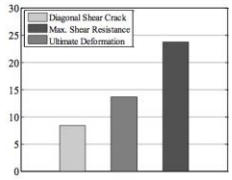	Specimen in this series showed limited response, the lateral strength suddenly dropped due to localized masonry wedge detachment. These specimens possessed high energy dissipation capacity, due to multiple diagonal cracks and low pre-compression.
W4	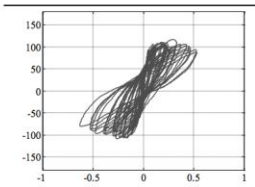	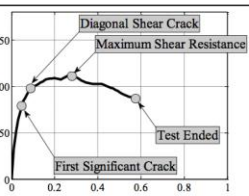	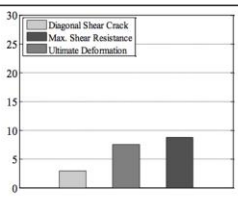	Specimen in this series showed limited response, the lateral strength suddenly dropped due to localized masonry crushing because of high pre-compression. These specimens possessed limited energy dissipation capacity, due to few diagonal cracks.

Fig. 4: Response of shear-dominated masonry walls under in-plane lateral quasi-static cyclic load

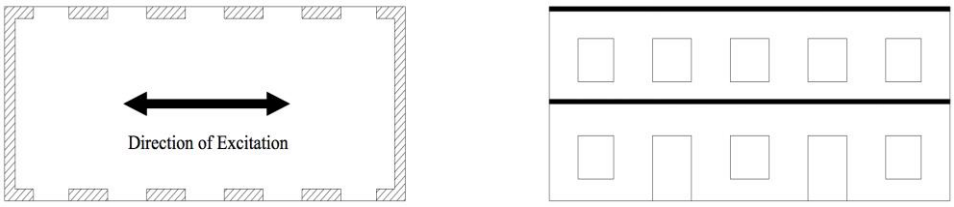

Fig. 5: Typical geometry and configuration of shear-dominated structures investigated in the present research study

As it has been observed in the experimental study that the aspect ratio and the pre-compression highly influence the lateral in-plane response parameters of shear-dominated walls. Thus, the mechanical properties of brick masonry material i.e. unit and mortar, and masonry walls obtained, as mentioned earlier, were considered in the design of randomly generated proto-type structures. The basic material properties were analyzed to retrieve the characteristic estimate of mechanical parameters required in the design of proto-type structures. Table 2 shows the characteristics of case study structures considered in the present research for investigation; it included a total of forty-nine combinations with varying wall density and floor areas; where wall density represents the ratio of total cross-section area of in-plane walls to the floor/covered area.

5. Numerical Modelling of Masonry Structures using Simplified Seismic Analysis

The method used for the numerical modelling and nonlinear dynamic time history analysis (NLTHA) of masonry structures in the present study was based on the equivalent frame idealization of masonry walls, called as equivalent frame method EFM, as proposed elsewhere (Galasco et al., 2002; Kappos et al., 2002; Magenes and Fontana, 1998; among others). The EFM was used for global performance evaluation of masonry structures using simplified hypothesis. In this modelling approach, a perforated wall was idealized as an equivalent frame that is modeled with beam-type frame element, as shown in Figure 6, which was provided with lumped plasticity inelastic hinges to simulate in-plane force-deformation constitutive behavior of walls.

Table 2. Geometric and material properties of structures investigated

S. No.	Wall Density (%)	Floor Area (m^2)	f_m (kN/m^2)	f_{tu} (kN/m^2)	E_m (MPa)	G_m (MPa)	γ (kN/m^3)
1	1.98	68.91					
2	2.55	85.87					
3	3.27	107.00					
4	4.20	133.33	3500	105	1225	490	18
5	5.39	166.14					
6	6.11	185.46					
7	6.92	207.02					

Moment-rotation constitutive law was assigned to the inelastic hinges of frame whereas shear-deformation constitutive law was assigned to the inelastic hinge of spandrel, as recommended (Magenes et al., 2000). On lateral translation the pier simulate the in-plane force-deformation behavior whereas the spandrel simulate the vertical shear-deformation response. A suitable constitutive law was desired for pier and spandrel to simulate the inelastic behavior of masonry wall.

Strength Models: The following strength models may be employed to provide estimate of the moment-resisting capacity of the frame-element nonlinear hinges, after Magenes and Calvi (1997), CEN (2004), NTC (2008), Turnsek and Sheppard (1980) and Tomazevic (1990).

Masonry Pier Strength Models

Toe Crushing: Increasing lateral force and deformation on in-plane walls tensile cracking of mortar at bed-joint takes place at the heel and the resistance is provided by the compressed toe of wall that ultimately show crushing and spalling of masonry. The corresponding ultimate strength can be obtained considering the couple produced by the axial load due to gravity and the compressive force corresponding to compression strength of compressed block of masonry at the toe.

$$M_f = \frac{pD^2t}{4\psi}\left(1-\frac{p}{kf_u}\right) \quad (3)$$

Diagonal Shear Cracking: An isotropic and homogeneous material attains shear strength corresponding to the onset of diagonal inclined cracks at the center of wall that takes place when the principal tensile stresses attain the level of the tensile strength of masonry. For this, the corresponding lateral shear strength can be obtained transforming diagonal tension strength to horizontal shear stress.

$$M_d = \frac{Hf_{tu}Dt}{2b}\sqrt{1+\frac{p}{f_{tu}}} \quad (4)$$

Diagonal Shear Sliding: masonry wall cracking that follows head- and bed-joint of walls is primarily resisted by the masonry bond strength (mortar-to-brick bond) that governs cohesion, and friction resistance arising from the sliding past movement along masonry head- and bed-joints.

$$M_s = \frac{DHt(1.5c+\mu p)}{2\left(1+3\frac{cH\psi}{pD}\right)} \quad (5)$$

$$k = \frac{1}{\left(1+\frac{2\Delta_y\mu}{\Delta_x}\right)} \quad (6)$$

where p represents the normal stress on wall due to axial load; D represents the wall length; t represents thickness of the wall; H represents the height of pier; f_u represents the compression strength of masonry; k represents the coefficient used to idealize the stress distribution at the compressed toe of the wall which is assumed as 0.85; ψ is 1.0 for a wall with cantilever boundary whereas 0.50 for a wall with fixed-fixed boundary condition; ft_u represents the principal tensile strength, also called diagonal tensile strength; b=1 for $H/D \leq 1$, $b=H/D$ for $1<H/D<1.5$, and b=1.5 for $1.5 \leq H/D$ after (Benedetti and Petrini, 1984); M_f represents the rotational resistance of moment-rotation plastic hinge of frame element to overturning for the flexure rocking mechanism; M_d represents the rotational resistance of moment-rotation plastic hinge of frame element to overturning for the diagonal shear mechanism; M_s represents the rotational resistance of moment-rotation plastic hinge of frame element to overturning for the sliding mechanism. Whenever these models are used, the minimum will be assigned to the inelastic hinge. The above models were employed in the design and modelling of the case study structure to ensure only shear-dominated mechanism of in-plane walls.

The following strength models may be employed to provide estimate of the vertical shear capacity of the frame-element nonlinear hinge for spandrel, after the current Italian Code (NTC, 2008). However more recent experimental and numerical studies have provided further

improved models, which can be used for building construction using timber flooring and arching technique for masonry walls coupling (Beyer and Mangalathu, 2014 & 2013; Beyer and Dazio, 2012; Beyer, 2012, among others).

Masonry Spandrel Strength Models

Diagonal Shear Damage: The strength of spandrel effectively bonded at both the ends develop shear cracking and diagonal shear damage corresponding to the diagonal tension strength of the masonry.

$$V_t = htf_{vo} \tag{7}$$

Flexure Cracking and Crushing at the Ends: The strength of spandrel in this case is based on the maximum compression resistance of masonry, generally considers the maximum resisting moment associated to the flexure mechanism in order to resist the horizontal compression actions in the spandrels.

$$V_P = \frac{N_P h}{l}\left(1 - \frac{N_P}{0.85 f_{hu} ht}\right) \tag{8}$$

V_t represents the vertical shear strength of spandrel effectively bonded at the ends with a lintel or rc ring beam at the top and bottom of the rc slab; h is the section height of the masonry spandrel; t is the thickness of the spandrel; fv_0 is the shear strength in the absence of compression on bed joints and can be taken as 2/3 of ft_u. VP represents the shear strength of spandrel that corresponds to the maximum resisting moment associated to the flexure mechanism in order to resist the tension action in the spandrel; N_P represents the minimum of the tensile strength of the horizontal element (e.g. lintel if any), and the value $0.4 f_{hu} ht$, where f_{hu} is the compression strength of masonry in the horizontal direction i.e. in the plane of wall. If a structure has rc ring beam that is considered as rigid except where openings are found on the top and bottom sides of the element.

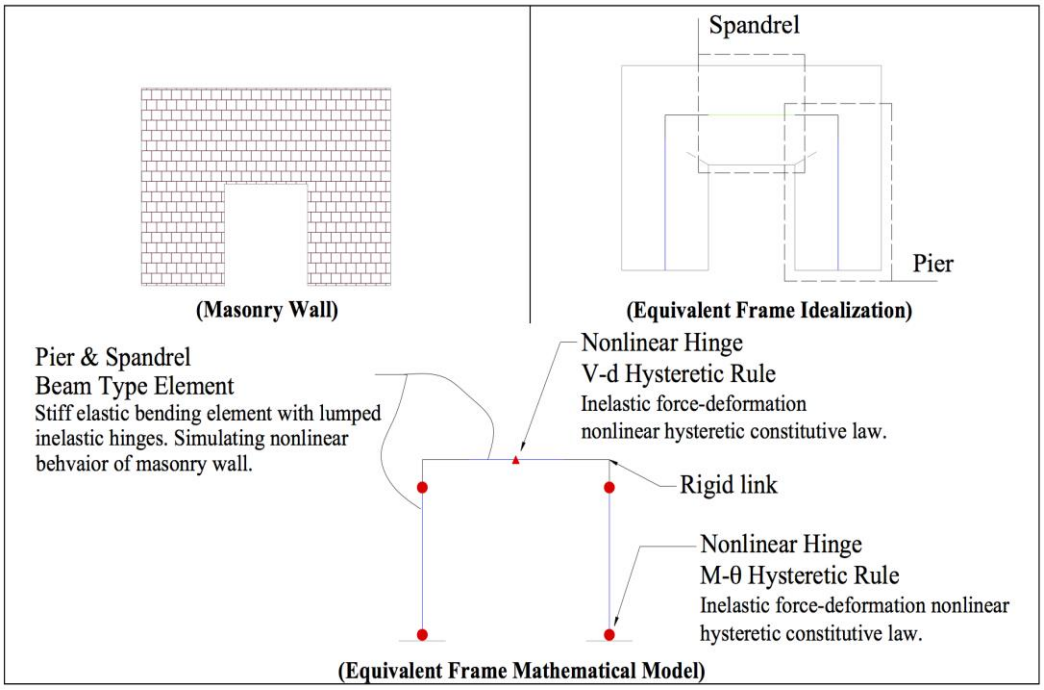

Fig. 6: Masonry wall mathematical modelling for nonlinear static and dynamic seismic analysis

Hysteretic Model: The force-deformation constitutive law of masonry wall can be selected based on the experimental data or available recommendations (Magenes and Calvi, 1997; Tomazevic, 1999). In the present study, the experimental investigation carried out on full-scale walls, as mentioned earlier, was considered to calibrate the moment-rotation hysteretic behavior of wall. Figure 7 shows the generalized assumed moment-rotation constitutive law of wall employed in the present study, which provide reasonable simulation of the experimentally obtained cyclic response of wall. The mathematical model for wall was prepared in OpenSees (McKenna et al., 2008), following the aforementioned mathematical modelling hypothesis (refer Figure 6).

The beam-column element used for masonry idealization is completely defined by masonry Young modulus, wall sectional area and the wall moment of inertia (50% reduced). The inelastic hinges are defined through Zerolength Element provided with Pinching Material, which are assigned with bi-linear moment-rotation hysteretic rule to simulate the in-plane force-deformation response of masonry wall, which is reasonable for

performance assessment of masonry structures (Ahmad et al., 2012). For calibration, the yield strength assigned to the nonlinear hinges is corresponding to the experimentally obtained maximum lateral strength reduced by ten percent whereas the yield drift corresponds to the idealized drift limit obtained from the experimental lateral force-displacement response as per recommendation of Magenes and Calvi (1997) and Tomazevic (1999). Figure 7 also shows a test dynamic seismic analysis of the wall under a natural acceleration time history record for 1994 Northridge earthquake.

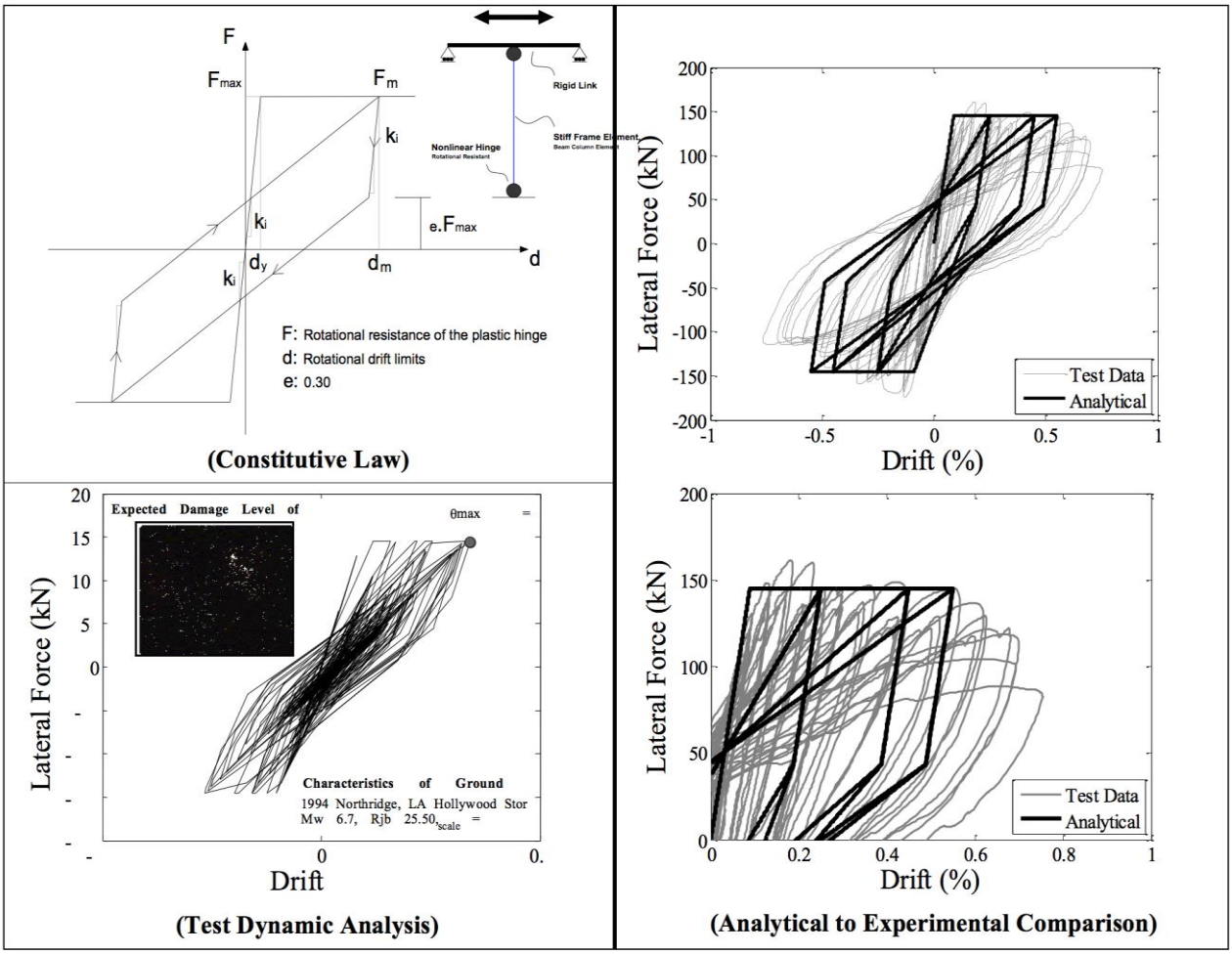

Fig. 7: Lateral force-deformation hysteretic response of tested masonry wall

It is worth to mention that the same constitutive law was not able to simulate reasonably the cyclic response of all tested walls (i.e. the hysteretic energy obtained experimentally), when considering variation in the aspect ratio and pre-compression level on the walls. Thus, calibration of the constitutive law is performed for all the tested walls (Figure 8) and a simplified relationship (model) was developed for the hysteretic rule parameter "*e*" whereby generalization of the constitutive law is now possible to walls of any geometry. It is observed that the parameter e is largely affected by the aspect ratio of wall and less affected by pre-compression (vertical loading) of wall.

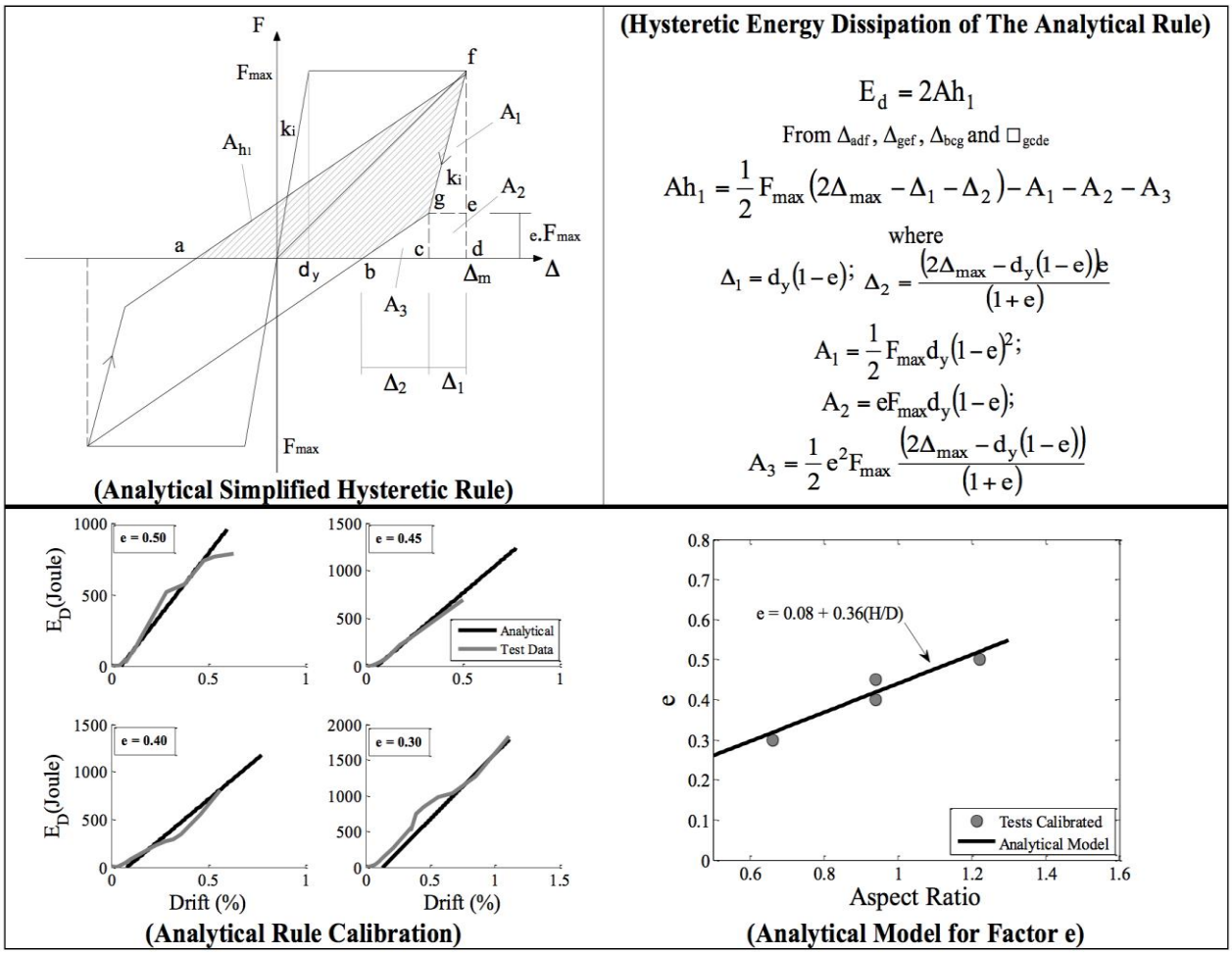

Fig. 8: Generalization of force-deformation hysteretic response of masonry walls.

6. Estimation of Ductility-Dependent R Factor

Ten natural accelerograms were extracted from the PEER NGA database for NLTHA of case study structures. The accelerograms were obtained for stiff soil condition with the mean spectrum compatible to BCP-2007 Type D soil spectrum.

In the first step, all the structures were analyzed statically through static pushover technique. It included the derivation of base shear and drift capacity curve under lateral loading. A constant load factor for ground storey mechanism, common for the considered structures, is employed with increased lateral drift demand. The objective of the analysis was to obtain the lateral strength and drift limits for each structure. The yield drift of the constitutive law for an in-plane wall is calculated dividing the wall shear strength over the wall lateral stiffness, considering both the shear and flexure deformation contribution of the wall.

The ultimate drift of an in-plane wall is computed using the analytical model for ductility capacity of wall derived from the experimental investigation on full-scale walls:

$$\mu = 6.0716 - 0.4078\sigma_0 \quad (9)$$

where μ represents the in-plane ultimate ductility capacity of masonry wall when the lateral strength reduced by 20 percent, generally recommended (Magenes and Calvi, 1997; Tomazevic, 1999); σ_0 (MPa) represents the pre-compression loading on walls. The identification code *Sij* employed for each case study structure represents a structure with wall density of case *i* and floor area of case *j* from Table 2.

In the next step, the structures were analyzed dynamically with the selected ten natural accelerograms scaled to multiple PGA levels in order to deform structure from elastic to inelastic state. The objective of this incremental dynamic analysis (IDA) was to derive structure response curve where structure inter-storey drift demand is correlated with shaking intensity. The linear scaling procedure adopted in the present study for NLTHA may provide bias estimate of structure's inter-storey drift demand due to the use of higher scaling factor (greater than 2), as compared to other selection and scaling procedures (Bommer and Acevedo, 2004). However, recent studies have shown that all scaling and matching criteria can provide reasonable estimate of the response of structure on average (Hancock et al., 2008) and even higher scaling factor may be employed (Watson-Lamprey and Abrahamson, 2006).

The computation of R factor herein was limited to the basic response modification factor of structure inherited by virtue of the ductility and energy dissipation capacity of structure whereas the contribution from over strength is not considered in the present study, due to the reason

mentioned earlier (refer Section 2.2). In the present study the concept of Kappos was extended to estimate the basic R factor, which was recently employed for other structures as well (Ali et al., 2012c, 2013; Kappos et al., 2011).

$$R = \frac{PGA_u}{PGA_y} \tag{10}$$

where PGA_u corresponds to the ground motions at the specified inter-storey ductility demand i.e. the PGA level whereby the structure will exceed the specified performance state; PGA_y corresponds to the ground motions level when the yield inter-storey drift of structure is reached. The above model is a modified version of the original proposal, in order to facilitate the computation. It is due to the fact that a constant amplification factor is encountered between the PGA and spectral acceleration at the fundamental vibration period of structure for both yield and ultimate limit states. The above concept is derived from the early proposal of Kappos (1991), which is proposed and employed by other researchers as well (Elnashai and Broderick, I9961; Mwafy and Elnashai, 2002). Figure 9 shows the framework employed for the estimation of R factor.

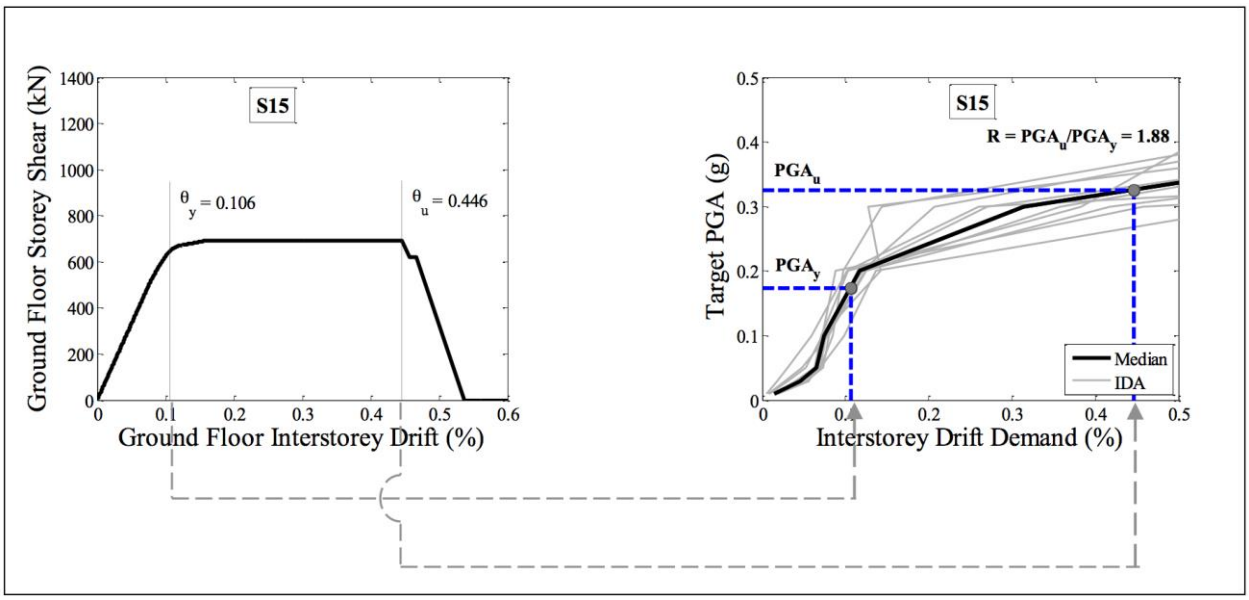

Fig. 9: Framework employed for the estimation of structure's R factor.

The idea of IDA of structures was to develop drift demand chart correlated with PGA. It is interpolated to identify the ground motions whereby the yield and ultimate drift capacity of structure is reached that are used to calculate R factor using Eq. (11). Figure 10 shows the estimated R factor for the considered shear-dominated brick masonry structures. A minimum R factor of 1.20 and maximum R factor of 2.74, with a mean R factor of 1.64 are observed for the considered unreinforced brick masonry shear-dominated structures. It is interesting to observe that the calculated ductility dependent R factor is in agreement with the BCP-SP 2007 specified R factor for masonry shear wall buildings.

Furthermore, the basic R factor obtained for the considered structures was correlated with some of the important structure's geometric and lateral response parameters like floor area, wall density and ductility capacity (considering also other specified ductility levels). Additionally, all the considered structures were also analyzed considering origin-centered hysteretic response (i.e. low energy dissipation) of masonry walls, which represents masonry structures with limited hysteretic energy dissipation that can be neglected in the analyses. Figure 11 shows the correlation of R factor with structure wall density and target ductility, and depicts also the effect of energy dissipation capacity of masonry wall on the correlation. Table 3 reports the basic R factor calculated for all the 49 structures considering four target ductility levels; 1.50, 2.0, 2.50 and 3.0 respectively.

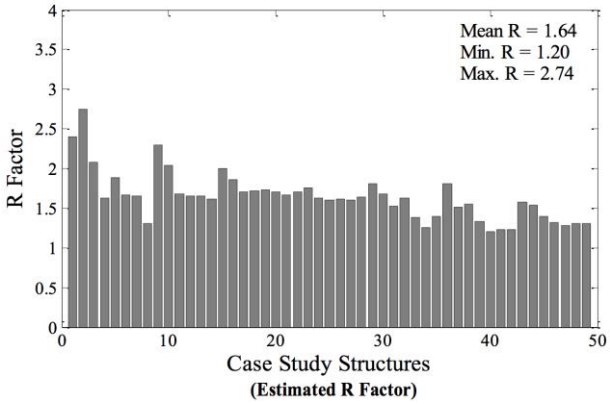

Fig. 10: Calculated basic response modification factor R, for unreinforced brick masonry shear-dominated structures in Pakistan

It can be observed that the target ductility, wall density (that result in high lateral strength and stiffness), floor area (that result in high pre-compression) and energy dissipation has significant influence on the basic R factor of shear-dominated masonry structures. It is worth to mention that

except the ductility capacity all other parameters are not considered in the current building code of Pakistan (BCP, 2007) like other most seismic design codes. For a given masonry typology (i.e. given the ductility capacity and nonlinear hysteretic response), the wall density and structural floor area affect the most structure's basic R factor. However, the influence of wall density on structure's R factor is relatively more than the floor area.

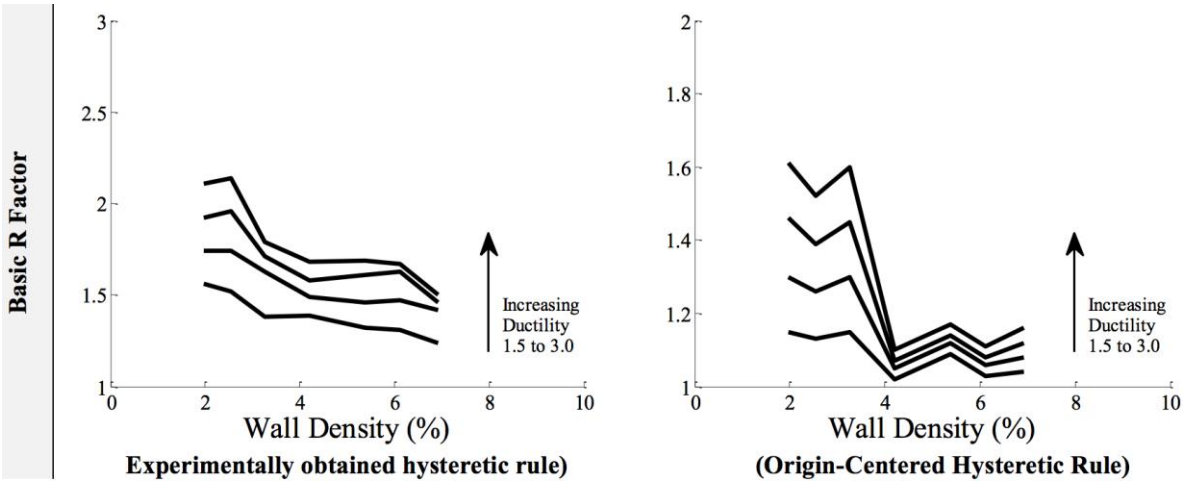

Fig. 11: The influence of wall density, target ductility and energy dissipation on the estimation of basic R factor for shear-dominated brick masonry structures.

Furthermore, the basic R factor was also calculated for all the above case study structures using the most common equation, as given below:

$$R = \sqrt{(2\mu - 1)} \tag{11}$$

where R was the basic response modification factor; μ represents the target ductility capacity of the structures. The R factor values computed using the above equation are compared with the dynamically obtained R factor and its percentage difference (i.e. underestimation/overestimation) was quantified for each case study structures (Figure 12). It can be observed that in the majority of cases (80% cases) the classical equation overestimates the basic R factor of shear-dominated structures investigated herein. The overestimation increases (as larger as 30%) for structures with high wall density and high ductility capacity. This merits the calculation of basic R factor through NLTHA using structure specific hysteretic behavior.

7. Conclusions

The paper presents the experimental and numerical investigation of low-rise (two-storey) unreinforced brick masonry shear-dominated structures, found in the northern areas of Pakistan. The experimental study included investigation on the masonry constituent materials for the characterization of basic mechanical properties. Additionally, it also included in-plane quasi-static cyclic tests on twelve (12) full-scale masonry walls for the characterization of important in-plane response parameters (e.g. in-plane shear strength, elastic and inelastic deformation limits, lateral force-deformation and hysteretic response). The numerical study included the development of numerical model to simulate the inelastic behavior of shear-dominated masonry walls, which was tested and validated against the experimentally tested full-scale walls. The numerical study was extended to perform nonlinear static pushover analysis and dynamic time history analysis of forty-nine (49) shear-dominated structures. The aim of the research work was to estimate the basic response modification factor R (ductility dependent R factor), which is proposed in the code specified static lateral load procedure for the design and assessment of structures. The outcome of the research is applicable to the considered low-rise unreinforced brick masonry shear-dominated structures that can ensure in-plane global seismic response and are governed by shear damages in masonry walls.
Furthermore, the following conclusions were drawn from the present study:

- The analysis performed on structures herein considered the material properties as the characteristic estimate of the values obtained from laboratory tests on considered masonry. These values have 95 percent chances of being exceeded in the tests.
- For the considered masonry structures the structural floor area, the total cross sectional area of in-plane walls to the floor area (wall density), ductility and energy dissipation affect mostly the structures' R factor and may correlate reasonably.
- For a given masonry typology, the lateral strength of structures increases with increase in wall density and/or floor area (whereby structures get stiffer) while the corresponding R factor decreases, for a given target ductility. However, among the two (i.e. structural floor area and wall density), wall density has relatively higher impact on the structure's R factor for the considered shear-dominated masonry structures.
- The Euro Code 8 specified basic R factor (behavior factor q) for unreinforced masonry structures (1.5 to 2.5) match reasonably well with the observed R factor (1.20 to 2.74) for the

considered shear-dominated masonry structures, considering maximum ductility of 3.

- The current building code of Pakistan recommend total R factor of 4.5, including over strength of 2.80, that result in basic R factor of 1.60, which is close to the mean estimate of 1.64.

Table 3. Basic R factor of shear-dominated masonry structures obtained for variety of prototype structures.

Floor Area (m^2)	Target Ductility	Wall Density (%)						
		1.98	**2.55**	**3.27**	**4.20**	**5.39**	**6.11**	**6.92**
69	1.50	1.53	1.53	1.63	1.32	1.33	1.43	1.32
	2.00	1.86	1.97	1.89	1.59	1.44	1.59	1.56
	2.50	2.19	2.05	2.16	1.67	1.54	1.75	1.61
	3.00	2.52	2.14	2.34	1.75	1.64	1.90	1.65
86	1.50	1.39	1.58	1.46	1.33	1.43	1.28	1.21
	2.00	1.77	1.75	1.64	1.50	1.57	1.43	1.37
	2.50	2.10	1.92	1.83	1.59	1.72	1.58	1.41
	3.00	2.18	2.08	1.90	1.69	1.86	1.63	1.45
107	1.50	1.65	1.56	1.31	1.37	1.32	1.31	1.22
	2.00	1.93	1.77	1.55	1.47	1.45	1.49	1.39
	2.50	2.03	1.98	1.62	1.56	1.58	1.60	1.42
	3.00	2.14	2.19	1.69	1.65	1.69	1.64	1.46
133	1.50	1.56	1.52	1.38	1.39	1.32	1.31	1.24
	2.00	1.74	1.74	1.63	1.49	1.46	1.47	1.42
	2.50	1.92	1.96	1.71	1.58	1.61	1.63	1.46
	3.00	2.11	2.14	1.79	1.68	1.69	1.67	1.50
166	1.50	1.65	1.34	1.25	1.39	1.31	1.34	1.17
	2.00	1.87	1.54	1.47	1.48	1.43	1.51	1.30
	2.50	2.10	1.74	1.54	1.57	1.55	1.66	1.41
	3.00	2.32	1.84	1.60	1.66	1.67	1.70	1.44
185	1.50	1.59	1.44	1.26	1.41	1.31	1.34	1.18
	2.00	1.78	1.67	1.50	1.50	1.44	1.56	1.34
	2.50	1.96	1.89	1.56	1.59	1.56	1.69	1.40
	3.00	2.15	2.03	1.63	1.68	1.68	1.73	1.44
207	1.50	1.69	1.49	1.28	1.43	1.26	1.30	1.27
	2.00	1.87	1.71	1.52	1.52	1.40	1.48	1.46
	2.50	2.06	1.93	1.58	1.61	1.54	1.63	1.53
	3.00	2.25	2.05	1.65	1.69	1.58	1.67	1.57

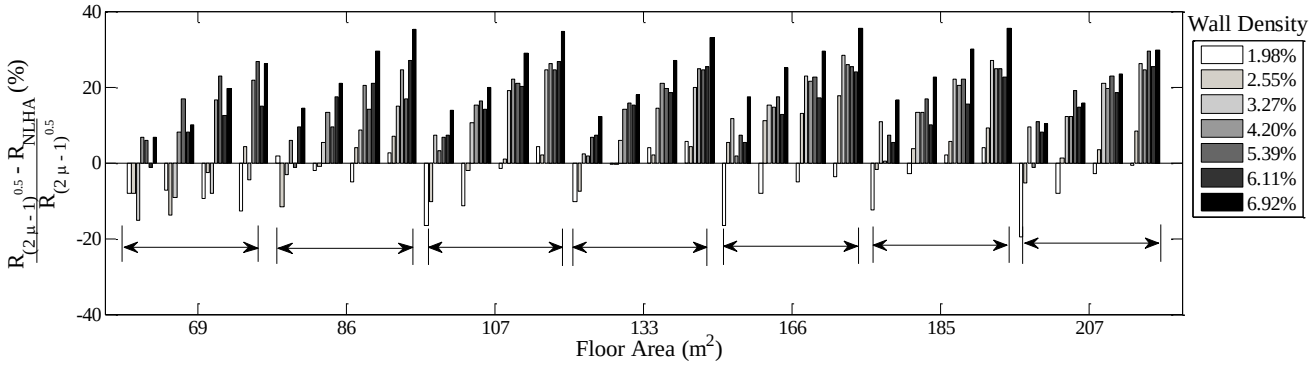

Fig. 12: Comparison of the dynamically obtained basic R factor with the R factor calculated using the ductility dependent classical equation used commonly

Acknowledgment.

The authors acknowledge and thank the Board of Advanced Studies and Research (BOASAR) and Higher Education Commission (HEC) of Pakistan for supporting the experimental studies conducted at the UET Peshawar by authors, which provided the basis for conducting the numerical research presented herein.

References

[1] Abram, D.P. (2001). Performance-based engineering concepts for unreinforced masonry building structures. Progress in Structural Engineering and Materials, Vol. 3, No. 1, pp. 48-56.

[2] Ahmad, N. (2015). A note on the strong ground motions and behavior of buildings during 26th Oct. 2015 Afghanistan-Pakistan earthquake. Technical Report, Earthquake Engineering Research Institute (EERI), Oakland, CA USA.

[3] Ahmad, N., Crowley, H., Pinho, R., Ali, Q., (2011). Frame-elements constitutive law for nonlinear static and dynamic analyses of masonry buildings. Contribution to Book Chapter "Masonry and Concrete Structures" In Cheung, S. O., Yazdani, S., Ghafoori, N. and Singh, A. (eds.) Modern Methods and Advances in Structural Engineering and Construction, Research Publishing Service, Singapore.

[4] Ali, Q. (2007). Case study of Pakistan housing reconstruction. Invited Seminar Lecture, ROSE School-IUSS Pavia, Pavia, Italy.

[5] Ali, Q. and Naeem, A. (2007). Seismic resistance evaluation of unreinforced masonry buildings. Journal of Earthquake Engineering, 11, 133-146.

[6] Ali, Q., Naeem, A., Ashraf, M., Ahmed, A., Alam, B., Ahmad, N., Fahim, M., Rahman, S., Umar, M. (2013). Seismic performance of stone masonry buildings used in the Himalayan Belt. Earthquake Spectra, 29, 1159-1181.

[7] Ali, Q., Badrashi, Y.I., Ahmad, N., Alam, B., Rehman, S. and Banori, F.A.S. (2012a). Experimental investigation on the characterization of solid clay brick masonry for lateral shear strength evaluation. International Journal of Earth Sciences and Engineering. 5, 782-791.

[8] Ali, Q., Naeem, A., Ahmad, N. and Alam, B. (2012b). In-Situ Dynamic Testing of Masonry Structure by Means of Underground Explosions Simulating Earthquake Motions, A Unique Case Study. International Journal of Earth Sciences and Engineering, 5, 1503-1534.

[9] Ali, Q., Schacher, T., Ashraf, M., Alam, B., Naeem, A., Ahmad, N. and Umar, M. (2012c). In-plane behavior of Dhajji-Dewari structural system (wooden braced frame with masonry infill). Earthquake Spectra, 28, 835-858.

[10] Alsuwwi, A.H., Hassan, M., Awwad, J. and Ahmad, N. (2015). Comparative analysis of cement-sand & cement-sand-khaka (stone dust) mortar shear wall brick masonry materials. Masonry International, Vol. 28(01), pp. 1-10.

[11] BCP (2007). Building Code of Pakistan–Seismic provision 2007. Technical Document, Ministry of Housing and Works, Islamabad, Pakistan.

[12] Benedetti, D. and Petrini, V. (1984). Sulla vulnerabilita di edifici in muratura: Proposta di un metodo di valutazione. LŠindustria delle Costruzioni, Vol. 149, No. 1 pp. 66–74.

[13] Beyer, K. and Mangalathu, S. (2014). Numerical Study on the Peak Strength of Masonry Spandrels with Arches. Journal of Earthquake Engineering, Vol. 18, No. 2, pp. 169-186.

[14] Beyer, K. and Mangalathu, S. (2013). Review of strength models for masonry spandrels. Bulletin of Earthquake Engineering, Vol. 11, pp. 521-542.

[15] Beyer, K. and Dazio, A. (2012). Quasi-static cyclic tests on masonry spandrels. Earthquake Specra, Vol. 28, No. 3, pp. 907-929.

[16] Beyer, K. (2012). Peak and residual strengths of brick masonry spandrels. Engineering Structures, Vol. 41, pp. 533-547.

[17] Bommer, J.J. and Acevedo, A.B. (2004). The use of real earthquake accelerograms as input to dynamic analyses. Journal of Earthquake Engineering, 8 (S1), 43-91.

[18] CEN. (1994) Eurocode8: Design provisions for earthquake resistance of structures. Part1–1: General rules–Seismic actions and general requirements for structures, prEN 1998-1-1, Comite Europeen de Normalisation, Brussels, Belgium.

[19] Dizhur, D., N. Ismail, and J. M. Ingham. (2010). Performance of unreinforced and reinforced masonry buildings during the 2010 Darfield earthquake. Bulletin of the New Zealand Society for Earthquake Engineering, Vol. 43(4), pp. 321–339.

[20] Dizhur, D., J. Ingham, L. Moon, M. Griffith, A. Schultz, I. Senaldi, G. Magenes, et al. (2011). Performance of masonry buildings and churches in the 22 February 2011 Christchurch earthquake. Bulletin of the New Zealand Society for Earthquake Engineering, Vol. 44(4), pp. 279–296.

[21] Elnashai, A. S. and Broderick, B. M. (I9961). Seismic response of composite frames - II. Calculation of behaviour factors. Engineering Structures, l8, 707-723.

[22] FEMA P-695 (2009). Quantification of building seismic performance factors. Federal Emergency Management Agency (FEMA), Washington, DC, USA.

[23] FEMA (2000). Pre-standard and commentary for the seismic rehabilitation of buildings. Federal Emergency Management Agency (FEMA), Washington, DC, USA.

[24] Galasco, A., Lagomarsino, S. and Penna, A. (2002). TREMURI Program: Seismic analyses of 3D masonry buildings. University of Genoa, Genoa, Italy.

[25] Hancock, J., Bommer, J.J. and Stafford, P.J. (2008). Numbers of scaled and matched accelerograms required for inelastic dynamic analyses. Earthquake Engineering and Structural Dynamics, 37, 1585-1607.

[26] Jackson, R. (1960). Thirty seconds at Quetta: The story of an earthquake. Evans Brothers Ltd., London, England.

[27] Jain, S.K. and Nigan, N.C. (2000). Historical developments and current status of earthquake engineering in India. Proceedings of the Twelfth World Conference on Earthquake Engineering, Auckland, New Zealand.

[28] Javed, M., Magenes, G., Alam, B., Khan, A. N., Ali, Q. and Ali, S. M. (2015). Experimental seismic performance evaluation of unreinforced brick masonry shear walls, Earthquake Spectra, Vol. 31, No. 1, pp. 215-246.

[29] Javed, M., Naeem, A. and Magenes, G. (2008). Performance of masonry structures during earthquake - 2005 in Kashmir. Mehran University Research Journal of Engineering & Technology, 27(3), 271-282.

[30] Kappos, A.J. (1999). Evaluation of behaviour factors on the basis of ductility and overstrength studies, Engineering Structures, 21(9), 823-835.

[31] Kappos, A.J. (1991). Analytical prediction of the collapse earthquake for r/c buildings: suggested methodology. Earthquake Engineering & Structural Dynamics, 20, 167-176.

[32] Kappos, A., Paraskeva, T., Moschonas, J. (2011). Evaluation of available force reduction factors for concrete bridges. Proceedings of the 9th US National and 10th Canadian Conference on Earthquake Engineering, Toronto, Canada.

[33] Kappos, A.J., Penelis, G.G., and Drakopoulos, C.G. (2002). Evaluation of simplified models for lateral load analysis of unreinforced masonry buildings, Journal of Structural Engineering, 128, 890-897.

[34] Klinger, R.E. (2004). Seismic behavior and design of masonry. In Bozorgnia, Y. and Bertero, V.V. (eds.): Earthquake Engineering: From engineering seismology to performance-based engineering, CRC Press, Florida, USA.

[35] Kumar, S.L. (1933). Theory of earthquake resisting design with a note on earthquake resisting construction in Baluchistan. Pakistan Engineering Congress, Paper No. 165, 154-189. (http://pecongress.org.pk/images/upload/books/Paper165.pdf)

[36] Magenes, G., Penna, A., Senaldi, I. E., Rota, M. and Galasco, A. (2013). Shaking Table Test of a Strengthened Full-Scale Stone Masonry Building with Flexible Diaphragms, International Journal of Architectural Heritage, Vol. 8 (3), pp. 349-375.

[37] Magenes, G. (2006). Masonry building design in seismic areas: Recent experiences and prospects from a European standpoint. Proceedings of the First European Conference on Earthquake Engineering and Seismology, Keynote 9, Geneva, Switzerland.
[38] Magenes, G. (2004). Prospettive per la revisione della normativa sismica nazionale con riguardo alle costruzioni in muratura, Assemblea ANDIL, sez. Murature, Isola Vicentina, Vicenza, Italy.
[39] Magenes, G., Bolognini, D., and Braggio, C. (2000). Metodi semplificati per l'analisi sismica non linear di edifici in muratura. Technical Report, CNR-Gruppo Nazionale per al Difesa dai Terremoti (GNDT), Roma, Italy.
[40] Magenes, G. and Morandi, P. (2008). Some issues on seismic design and assessment of masonry buildings based on linear elastic analysis. Proceedings of the Michael John Nigel Priestley Symposium, IUSS Press, Pavia, Italy.
[41] Magenes, G. and Fontana, D. (1998). Simplified non-linear seismic analysis of masonry buildings, Proceedings of the British Masonry Society, 8, 190-195.
[42] Magenes, G., and Calvi, G.M. (1997). In-plane seismic response of brick masonry walls, Earthquake Engineering and Structural Dynamics, Vol. 26, No. 11, pp. 1091-1112.
[43] Mahmoudi, M. and Mahdi, Z. (2013). Determination the response modification factors of buckling restrained braced frames. Proceedia Engineering, Vol. 54, pp. 222-231.
[44] Mann, W. and Muller, H. (1982). Failure of shear-stressed masonry-An enlarge theory, tests and application to shear walls. Proceedings of the British Ceramic Society, 30, 223.
[45] Masoudi, M., Eshghi, S., Ghafory-Ashtiany, M. (2012). Evaluation of response modification factor (R) of elevated concrete tanks. Engineering Structures, Vol.39, pp. 199-209.
[46] McKenna, F., Fenves, G.L. and Scott, M.H. (2010). Open System for Earthquake Engineering Simulation: Version2.1.0, University of California Berkeley, California, USA.
[47] Menon, A. and Magenes, G. (2011). Definition of seismic input for out-of-plane response of masonry walls: II. Formulation. Journal of Earthquake Engineering, 15, 195-213.
[48] Miranda, E. (1997). Strength reduction factors in performance-based design, EERC-CUREe Symposium in Honor of Vitelmo V. Bertero, Berkeley, CA, USA.
[49] Morandi, P. and Magenes, G. (2008). Seismic design of masonry buildings: Current procedures and new perspectives, Proceedings of the Fourteenth World Conference on Earthquake Engineering, Beijing, China.
[50] Mwafy, A.M. and Elnashai, A.S. (2002). Calibration of force reduction factors of rc buildings, Journal of Earthquake Engineering, 6, 239-273.
[51] Murthy, C.V.R. (2003). How do brick masonry houses behave during earthquakes?. In EQTips – Learning Earthquake Design and Construction, Indian Institute of Technology, Kanpur, India.
[52] Naeem, A. et al. (1996). A Research Project on Khaka – Undergraduate research work at the Department of Civil Engineering, University of Engineering and Technology, Peshawar, KP Pakistan.
[53] NTC (2008). Approvazione delle nuove norme tecniche per le costruzioni, Gazzetta Ufficiale della Repubblica Italiana, n. 29 del 4 Febbraio 2008 – Suppl. Ordinario n. 30. (In Italian). (http://www.cslp.it/cslp/index.php?option=com_docman&task=doc_download&gid=3269&Itemid=10).
[54] Peiris, N., Rossetto, T., Burton, P., and Mahmood, S. (2008). EEFIT Mission: October 8, 2005 Kashmir earthquake. Technical Report, Earthquake Engineering Field Investigation Team, Institution of Structural Engineers, London, United Kingdom.
[55] Penna, A., Senaldi, I.E., Galasco, A. and Magenes, G. (2015). Numerical simulation of shaking table tests on full-scale stone masonry buildings. International Journal of Architectural Heritage, Vol. 10(2-3), pp. 146-163.
[56] Porto, F.D., Grendene, M. and Modena, C. (2009). Estimation of load reduction factors for clay masonry walls. Earthquake Engineering and Structural Dynamics, 38, 155-1174.
[57] Priestley, M.J.N., Calvi, G.M., and Kowalsky, M.J. (2007). Displacement-Based Seismic Design of Structures, IUSS Press, Pavia, Italy.
[58] Rai, D.C. (2002). Review of design codes for masonry buildings. Indian Institute of Technology, Kanpur, India.
[59] Rossetto, T. and Peiris, N. (2009). Observations of damage due to the Kashmir earthquake of October 8, 2005 and study of current seismic provisions for buildings in Pakistan. Bulletin of Earthquake Engineering, 7(3), 681-699.
[60] Senaldi, I., Magenes, G. and Ingham, J. (2015). Damage assessment of unreinforced stone masonry buildings after the 2010-2011 Canterbury earthquakes. International Journal of Architectural Heritage, Vol. 9(5). pp. 605-627.
[61] Senaldi, I., Magenes, G., Penna, A., Galasco, A. and Rota, M. (2014). The effect of stiffened floor and roof diaphragms on the experimental seismic response of a full-scale unreinforced stone masonry building. Journal of Earthquake Engineering, Vol. 18(3). pp. 407-443.
[62] Shahzada K, Khan, A. N., Elnashai A. S., Ashraf M, Javed M, Naseer A, Alam B (2012). Experimental seismic performance evaluation of unreinforced brick masonry buildings. Earthquake Spectra, Vol. 28, No. 3, pp. 1269-1290.
[63] Shahzada K, Khan, A. N., Elnashai A. S., Naseer, A., Javed, M., Naseer, Ashraf, M. (2012). Shake table test of confined brick masonry building. Advanced Material Research, Vol. 255-260, pp. 689-693. DOI: 10.4028/www.scientific.net/AMR.255-260.689
[64] Tomazevic, M. (1990). Masonry structures in seismic areas– a state-of-the-art report. Proceedings of the 9th European Conference on Earthquake Engineering, Moscow, A, 246-302.
[65] Tomazevic, M. (1999). Earthquake-Resistant Design of Masonry Buildings-Innovation in Structures and Construction Vol. 1, Imperial College Press, London, UK.
[66] Turnsek, V. and Sheppard, P. (1980). The shear and flexural resistance of masonry walls. Proceedings of the International Research Conference on Earthquake Engineering, Skopje, 517-573.
[67] Vasconcelos, G. and Lourenco, P. B. (2009). In-Plane experimental behavior of stone masonry walls under cyclic loading, Journal of Structural Engineering, Vol. 135, No. 10, pp. 1269-1277.
[68] Watson-Lamprey, J. and Abrahamson, N. (2006). Selection of ground motion time series and limits on scaling. Soil Dynamics and Earthquake Engineering, 26, 477-482.